

# Lawrence Berkeley National Laboratory

LBL Publications

## Title

Transverse momentum resummation for t-channel single top quark production at the LHC

## Permalink

<https://escholarship.org/uc/item/9rw7g95t>

## Journal

Physical Review D, 98(5)

## ISSN

2470-0010

## Authors

Cao, Qing-Hong

Sun, Peng

Yan, Bin

et al.

## Publication Date

2018-09-01

## DOI

10.1103/physrevd.98.054032

Peer reviewed

## Transverse momentum resummation for $t$ -channel single top quark production at the LHC

Qing-Hong Cao,<sup>1,2,3,\*</sup> Peng Sun,<sup>4,5,†</sup> Bin Yan,<sup>1,4,‡</sup> C.-P. Yuan,<sup>4,§</sup> and Feng Yuan<sup>6,||</sup>

<sup>1</sup>*Department of Physics and State Key Laboratory of Nuclear Physics and Technology, Peking University, Beijing 100871, China*

<sup>2</sup>*Collaborative Innovation Center of Quantum Matter, Beijing 100871, China*

<sup>3</sup>*Center for High Energy Physics, Peking University, Beijing 100871, China*

<sup>4</sup>*Department of Physics and Astronomy, Michigan State University, East Lansing, Michigan 48824, USA*

<sup>5</sup>*Department of Physics and Institute of Theoretical Physics, Nanjing Normal University, Nanjing, Jiangsu, 210023, China*

<sup>6</sup>*Nuclear Science Division, Lawrence Berkeley National Laboratory, Berkeley, California 94720, USA*



(Received 4 February 2018; published 28 September 2018)

We study the effect of multiple soft gluon radiation on the kinematical distributions of the  $t$ -channel single top quark production at the LHC. By applying the transverse momentum-dependent factorization formalism, large logarithms (of the ratio of large invariant mass  $Q$  and small total transverse momentum  $q_{\perp}$  of the single-top plus one-jet final state system) are resummed to all orders in the expansion of the strong interaction coupling at the accuracy of the next-to-leading logarithm, including the complete next-to-leading-order corrections. We show that the main difference from PYTHIA prediction lies in the inclusion of the exact color coherence effect between the initial and final states in our resummation calculation, which becomes more important when the final state jet is required to be in the forward region. We further propose to apply the experimental observable  $\phi^*$ , similar to the one used in analyzing precision Drell-Yan data, to test the effect of multiple gluon radiation in the single-top events. The effect of the bottom quark mass is also discussed.

DOI: [10.1103/PhysRevD.98.054032](https://doi.org/10.1103/PhysRevD.98.054032)

### I. INTRODUCTION

The top quark is the heaviest particle of the standard model (SM) of elementary particle physics, with its mass around the electroweak symmetry breaking scale. It is believed that studying its detailed interactions could shed light on possible new physics beyond the SM. Furthermore, the lifetime of the top quark is much smaller than the typical hadronization time scale, so that one can also determine the properties (including polarization) of this heavy bare quark, produced from various scattering processes, by studying the kinematical distributions of the top quark and its decay particles. Top quarks are predominantly produced in pairs through gluon fusion process, via strong interaction, at the

CERN Large Hadron Collider (LHC). It can also be produced singly via charged-current electroweak interaction, involving a  $Wtb$  coupling [1–4], which offers a promising way to precisely study the  $Wtb$  coupling and the  $V_{tb}$  Cabibbo-Kobayashi-Maskawa (CKM) matrix element.

To test the  $Wtb$  coupling of the top quark from measuring the production rate of single-top events, one has to be able to precisely predict the detection efficiency of the events after imposing needed kinematic cuts. Hence, higher-order calculations are required. The single top quark production and decay in hadron collision at the next-to-leading-order (NLO) and next-to-next-to-leading-order (NNLO) accuracy in QCD correction have been discussed widely. (See Ref. [5], and the references therein). To go beyond the fixed-order calculations, the threshold resummation technique has been applied to improve the prediction on the single-top inclusive production rate at the next-to-leading-logarithm (NLL) and next-to-next-to-leading-logarithm (NNLL) accuracy [6–11]. The threshold resummation technique has also been used to improved the prediction on the transverse momentum distribution of the top quark by summing over large logarithms  $\ln(m_t^2/s_4)$  with  $s_4 \rightarrow 0$ , where  $s_4 = \hat{s} + \hat{t} + \hat{u} - m_t^2$ ,  $\hat{s}$ ,  $\hat{t}$  and  $\hat{u}$  are the usual Mandelstam variables [6–11].

\* qinghongcao@pku.edu.cn

† pengsun@msu.edu

‡ yanbin1@msu.edu

§ yuan@pa.msu.edu

|| fyuan@lbl.gov

Published by the American Physical Society under the terms of the [Creative Commons Attribution 4.0 International license](https://creativecommons.org/licenses/by/4.0/). Further distribution of this work must maintain attribution to the author(s) and the published article's title, journal citation, and DOI. Funded by SCOAP<sup>3</sup>.

In this article, we focus on improving the prediction on the kinematical distributions of  $t$ -channel single top events, by applying the transverse momentum resummation formalism to sum over large logarithms  $\ln(Q^2/q_\perp^2)$ , with  $Q \gg q_\perp$ , to all orders in the expansion of the strong interaction coupling at the NLO-NLL accuracy, where  $Q$  and  $q_\perp$  are the invariant mass  $Q$  and total transverse momentum  $q_\perp$  of the single-top plus one-jet final state system, respectively. We adopt the  $q_\perp$  resummation formalism based on the transverse momentum-dependent (TMD) factorization formalism [12], which has been widely discussed in the literature to resum this sort of large logarithms in the color singlet processes, such as the Drell-Yan pair production [13,14]. The application of the  $q_\perp$  resummation formalism for processes with more complicated color structures, such as heavy quark production, was firstly discussed in Refs. [15–17]. For processes involving massless jets in the final state, the  $q_\perp$  resummation formalism needs to be further modified to take into account the color coherence effect induced by the presence of the light (quark and gluon) jets in the final state [18–23]. The extra soft gluon radiations in the event could be either within or outside the observed final-state jet cone. Within the jet cone, the radiated gluon is treated as collinear to the final state parton, and it leads to a contribution to the bin of  $q_\perp = 0$ . This contribution can be factorized out as a jet function based on the TMD resummation formalism [20]. When outside of observed final-state jet cone, the radiated soft gluon will generate a nonvanishing  $q_\perp$ , and induce the large logarithms  $\ln(Q^2/q_\perp^2)$  which needs to be resummed via the *modified*  $q_\perp$  resummation formalism.

The experimental signature of the  $t$ -channel single top event at the LHC is an energetic light jet, associatively produced with the single top quark, in the final state. As to be shown below, the location and height of the Sudakov peak,

in the  $q_\perp$  distribution of  $t$ -channel single top events, strongly depends on the color coherence effect, induced by soft gluon interaction between the initial and final state jets, and the treatment of bottom quark mass in the resummation calculation. The (formally) subleading logarithms play an important role when the final state jet is required to be in the forward region, where our resummation prediction is noticeably different from the PYTHIA parton shower result.

## II. RESUMMATION FORMALISM

We consider the process  $pp \rightarrow t + jet + X$  at the LHC. Using the TMD resummation formalism presented in Ref. [20], the differential cross section of the  $t$ -channel single top quark production process can be summarized as

$$\frac{d^4\sigma}{dy_t dy_J dP_{J\perp}^2 d^2q_\perp} = \sum_{ab} \left[ \int \frac{d^2\vec{b}}{(2\pi)^2} e^{-i\vec{q}_\perp \cdot \vec{b}} W_{ab \rightarrow tJ}(x_1, x_2, \mathbf{b}) + Y_{ab \rightarrow tJ} \right], \quad (1)$$

where  $y_t$  and  $y_J$  are the rapidities for the top quark and the final state jet, respectively;  $P_{J\perp}$  and  $q_\perp$  are the transverse momenta of the jet and the total transverse momentum of the top quark and the jet system, i.e.,  $\vec{q}_\perp = \vec{P}_{t\perp} + \vec{P}_{J\perp}$ . The  $W_{ab \rightarrow tJ}$  term contains all-order resummation contributions, in powers of  $\ln(Q^2/q_\perp^2)$ , and the inclusion of the  $Y_{ab \rightarrow tJ}$  term is to account for the missing (nonsingular) part of the fixed-order correction when expanding the  $W_{ab \rightarrow tJ}$  term to the same order in the strong coupling constant  $g_s$  as the fixed-order calculation. The variables  $x_1, x_2$  are momentum fractions of the incoming hadrons carried by the two incoming partons.

The above  $W$  term can be further written as

$$W_{ab \rightarrow tJ}(x_1, x_2, \mathbf{b}) = x_1 f_a(x_1, \mu_F = b_0/b_*) x_2 f_b(x_2, \mu_F = b_0/b_*) e^{-S_{\text{Sud}}(Q^2, \mu_{\text{Res}}, b_*)} e^{-\mathcal{F}_{NP}(Q^2, \mathbf{b})} \times \text{Tr} \left[ \mathbf{H}_{ab \rightarrow tJ}(\mu_{\text{Res}}) \exp \left[ - \int_{b_0/b_*}^{\mu_{\text{Res}}} \frac{d\mu}{\mu} \boldsymbol{\gamma}^{s\dagger} \right] \mathbf{S}_{ab \rightarrow tJ}(b_0/b_*) \exp \left[ - \int_{b_0/b_*}^{\mu_{\text{Res}}} \frac{d\mu}{\mu} \boldsymbol{\gamma}^s \right] \right], \quad (2)$$

where  $Q^2 = \hat{s} = x_1 x_2 S$ ,  $b_0 = 2e^{-\gamma_E}$ ,  $f_{a,b}(x, \mu_F)$  are parton distribution functions (PDF) for the incoming partons  $a$  and  $b$ , and  $\mu_{\text{Res}}$  represents the resummation scale of this process. Here, we define  $b_* = \mathbf{b} / \sqrt{1 + \mathbf{b}^2/b_{\text{max}}^2}$  with  $b_{\text{max}} = 1.5 \text{ GeV}^{-1}$ , which is introduced to factor out the nonperturbative contribution  $e^{-\mathcal{F}_{NP}(Q^2, \mathbf{b})}$ , arising from the large  $\mathbf{b}$  region (with  $\mathbf{b} \gg b_*$ ) [24–26]. In this study, we shall use CT14NNLO PDFs [27] for our numerical calculation. Hence, our resummation calculation should be consistently done in the General-Mass-Variable-Flavor (GMVF) scheme in which the PDFs are determined. The bottom quark PDF is set to zero when the factorization

scale  $\mu_F$  is below the bottom quark mass  $m_b$ . To properly describe the small  $q_\perp$  region (for  $q_\perp < m_b$ ), the S-ACOT scheme [28–31] is adopted to account for the effect from the (nonzero) mass of the incoming bottom quark in the hard scattering process  $qb \rightarrow q't + X$ . In Refs. [32–34], a detailed discussion has been given on how to implement the S-ACOT scheme in the  $q_\perp$  resummation formalism, for processes initiated by bottom quark scattering. In short, the S-ACOT scheme retains massless quark in the calculation of the hard scattering amplitude (of  $qb \rightarrow q't$ ), but with the (bottom quark) mass-dependent Wilson coefficient  $C_{b/g}^{(1)}(x, \mathbf{b}, \mu_F)$ , to account for the contribution from gluon

splitting into a  $b\bar{b}$  pair [32–34]. The hard and soft factors  $\mathbf{H}$  and  $\mathbf{S}$  are expressed as matrices in the color space of  $ab \rightarrow tJ$ , and  $\gamma^s$  is the associated anomalous dimension for the soft factor. The Sudakov form factor  $\mathcal{S}_{\text{Sud}}$  resums the leading double logarithm and the subleading logarithms, and is found to be

$$\mathcal{S}_{\text{Sud}}(Q^2, \mu_{\text{Res}}, b_*) = \int_{b_0^2/b_*^2}^{\mu_{\text{Res}}^2} \frac{d\mu^2}{\mu^2} \left[ \ln\left(\frac{Q^2}{\mu^2}\right) A + B + D_1 \ln \frac{Q^2 - m_t^2}{P_{J\perp}^2 R^2} + D_2 \ln \frac{Q^2 - m_t^2}{m_t^2} \right], \quad (3)$$

where  $R$  represents the cone size of the final state jet,  $m_t$  is the top quark mass. Here, the parameters  $A$ ,  $B$ ,  $D_1$  and  $D_2$  can be expanded perturbatively in  $\alpha_s$ , which is  $g_s^2/(4\pi)$ . At one-loop order,

$$A = C_F \frac{\alpha_s}{\pi}, \quad B = -2C_F \frac{\alpha_s}{\pi}, \quad D_1 = D_2 = C_F \frac{\alpha_s}{2\pi}, \quad (4)$$

with  $C_F = 4/3$ . In our numerical calculation, we will also include the  $A^{(2)}$  contribution since it is associated with the incoming parton distributions and universal for all processes initiated by the same incoming partons. The cone size  $R$  is introduced to regulate the collinear gluon radiation associated with the final state jet [18–23].

The soft gluon radiation can be factorized out based on the Eikonal approximation method. For each incoming or outgoing color particle, the soft gluon radiation is factorized into an associated gauge link along the particle momentum direction. The color correlation between the color particles in this process can be described by a group of orthogonal color bases. For the  $t$ -channel single top quark production, there are two orthogonal color configurations, which are

$$C_{1kl}^{ij} = \delta_{ik}\delta_{jl}, \quad C_{2kl}^{ij} = T_{ik}^{a'} T_{jl}^{a'}, \quad (5)$$

where  $i, j$  are color indices of the two incoming partons,  $k, l$  are color indices of the jet and the top quark in final states and  $a'$  is color index of the gluon. We follow the procedure of Ref. [20] to calculate the soft factor. Its definition in such color basis can be written as

$$S_{IJ} = \int_0^\pi \frac{d\phi}{\pi} C_{ii'}^{bb'} C_{jj'}^{aa'} \langle 0 | \mathcal{L}_{vcb'}^\dagger(b) \mathcal{L}_{\bar{v}bc'}(b) \mathcal{L}_{\bar{v}a'}^\dagger(0) \times \mathcal{L}_{vac}(0) \mathcal{L}_{nji}^\dagger(b) \mathcal{L}_{\bar{n}i'k}(b) \mathcal{L}_{\bar{n}kl}^\dagger(0) \mathcal{L}_{n'lj}(0) | 0 \rangle, \quad (6)$$

where we integrated out the azimuthal angle of the top quark and traded the relative azimuthal angle  $\phi$  for the  $q_\perp$ .  $I$  and  $J$  represent the color basis index,  $n$  and  $\bar{n}$  represent the

momentum directions of the top quark and the jet in this process,  $v$  and  $\bar{v}$  are the momentum directions of the initial states.

The anomalous dimension of the soft factor  $S_{IJ}$  can be calculated at one-loop order and found to be

$$\gamma^S_{ub \rightarrow dt} = \frac{\alpha_s}{\pi} \left[ \begin{array}{cc} C_F T & C_F/C_A U \\ U & \frac{1}{2}(C_A - 2/C_A)U - \frac{1}{2C_A}T \end{array} \right], \quad (7)$$

where,

$$T = \ln\left(\frac{-\hat{t}}{\hat{s}}\right) + \ln\left(\frac{-(\hat{t} - m_t^2)}{\hat{s} - m_t^2}\right), \quad (8)$$

$$U = \ln\left(\frac{-\hat{u}}{\hat{s}}\right) + \ln\left(\frac{-(\hat{u} - m_t^2)}{\hat{s} - m_t^2}\right). \quad (9)$$

Here  $C_A = 3$ ,  $\hat{t} = (p_u - p_d)^2$ ,  $\hat{u} = (p_b - p_d)^2$  for the  $ub \rightarrow dt$  process.

The hard factor  $H_{IJ}$  contains the contribution from the jet function which is proportional to the leading-order cross section. The jet function accounts for contribution originated from collinear gluon radiation, and is dependent on the jet algorithm used in the calculation. In this work, we apply the anti- $k_T$  jet algorithm, as discussed in Refs. [20,35].

Before concluding this section, we would like to point out that we did not include in this work the possibility of nonglobal logarithms [36–39]. The nonglobal logarithms (NGLs) arise from some special kinematics of two soft gluon radiations, in which the first one is radiated outside of the jet which subsequently radiates a second gluon into the jet. We have roughly estimated its numerical effect and found that the NGLs are negligible in this process since it starts at  $\mathcal{O}(\alpha_s^2)$  [40]. Therefore, we will ignore their contributions in the following phenomenology discussion.

### III. PHENOMENOLOGY

Below, we present the numerical result of resummation calculation for the  $t$ -channel single top quark production at the  $\sqrt{s} = 13$  TeV LHC with CT14NNLO PDF [27]. Figure 1 shows the  $q_\perp$  distribution from the asymptotic piece (blue dashed line), NLO calculation (red dotted line), resummation prediction (black solid line) and  $Y$ -term (orange dot-dashed line) for the top quark production. Here, the asymptotic piece is the fixed-order expansion of Eq. (1) up to the  $\alpha_s$  order, and is expected to agree with the NLO prediction as  $q_\perp \rightarrow 0$ . In the same figure, we also compare to the prediction from the parton shower event generator PYTHIA 8 [41] (green solid line), which was calculated at the leading order, with CT14LO PDF and  $\alpha_s(M_Z) = 0.118$  at the  $Z$ -boson mass scale (91.118 GeV). For the fixed-order calculation, both the renormalization and factorization scales are fixed at  $H_T \equiv \sqrt{m_t^2 + P_{J\perp}^2} + P_{J\perp}$ . Similarly, in the resummation calculation, the canonical

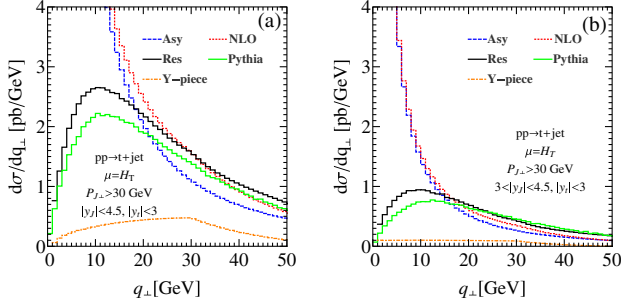


FIG. 1. The  $q_{\perp}$  distribution from the asymptotic result (blue dashed line), NLO calculation (red dotted line), resummation prediction (black solid line), parton shower result by PYTHIA 8 (green solid line) and  $Y$ -term (orange dot-dashed line) for the  $t$ -channel single top quark production at the  $\sqrt{S} = 13$  TeV LHC with  $|y_t| < 3$  and  $|y_J| \leq 4.5$  (a), or  $3.0 \leq |y_t| \leq 4.5$  (b). The resummation and renormalization scales are choose as  $\mu = \mu_{\text{Res}} = \mu_{\text{ren}} = H_T$ .

choice of the resummation ( $\mu_{\text{Res}}$ ) and renormalization ( $\mu_{\text{ren}}$ ) scales is taken to be  $H_T$  in this study. The jet cone size is taken to be  $R = 0.4$ , using the anti- $k_T$  algorithm, and the Wolfenstein CKM matrix element parameterization is used in our numerical calculation [42]. We shall compare predictions for two different sets of kinematic cuts, with  $|y_t| \leq 3$  and  $P_{J\perp} > 30$  GeV, and  $|y_J| \leq 4.5$  in (a), and  $3 \leq |y_t| \leq 4.5$  in (b) of Fig. 1, respectively. Some results of the comparison are in order. Clearly, the asymptotic piece and the fixed-order calculation results agree very well in the small  $q_{\perp}$  (less than 1 GeV) region. As a further check, we calculated the NLO total cross section predicted by our resummation calculation. Specifically, we numerically integrated out the  $q_{\perp}$  distribution predicted by our resummation calculation from 0 to 1 GeV, and summed it up with the integration of the perturbative piece (at the  $\alpha_s$  order) from 1 GeV up to the allowed kinematic region [43]. We found that the NLO total cross section predicted by our resummation framework and MCFM [44] calculations are in perfect agreement.

As shown in Fig. 1, the NLO prediction is not reliable when the  $q_{\perp}$  is small. The resummation calculation predicts a well behavior  $q_{\perp}$  distribution in the small  $q_{\perp}$  region since the large logarithms have been properly resummed. In Fig 2 (a), we compare the predictions from our resummation calculation to PYTHIA by taking the ratio of their  $q_{\perp}$  differential distributions shown in Fig. 1. With the jet rapidity  $|y_J| \leq 4.5$  (blue dashed line), this ratio does not vary strongly with  $q_{\perp}$ . Hence, they predict almost the same shape in the  $q_{\perp}$  distribution, while they predict different fiducial total cross sections because PYTHIA prediction includes only the leading-order matrix element and is calculated with CT14LO PDFs. However, if we require the final state jet to be in the forward rapidity region, with  $3 \leq |y_J| \leq 4.5$  (red solid line), which is the so-called signal region of single top events, we find that PYTHIA prediction disagrees with our resummation calculation.

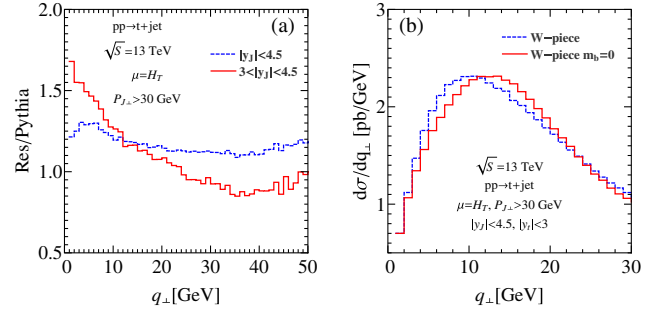


FIG. 2. (a) The ratio of the resummation and PYTHIA prediction for the  $t$ -channel single top quark production at the  $\sqrt{S} = 13$  TeV LHC with  $|y_t| < 3$ ,  $P_{J\perp} > 30$  GeV and  $|y_J| \leq 4.5$  (blue dashed line), or  $3.0 \leq |y_t| \leq 4.5$  (red solid line); (b) The  $W$ -piece prediction for the single top quark production process with  $m_b = 4.75$  GeV (blue dashed line) and  $m_b = 0$  (red solid line) at the  $\sqrt{S} = 13$  TeV LHC with  $|y_J| \leq 4.5$ ,  $|y_t| < 3$  and  $P_{J\perp} > 30$  GeV. The resummation and renormalization scales are choose as  $\mu = \mu_{\text{Res}} = \mu_{\text{ren}} = H_T$ .

Our resummation calculation predicts a smaller  $q_{\perp}$  value when the final state jet is required to fall into the forward region. We have checked that the PYTHIA result is not sensitive to the effects from beam remnants. Furthermore, the  $Y$ -term contribution, from NLO, is negligible in this region, cf. Fig. 1(b) (orange dot-dashed line). Hence, we conclude that their difference most likely comes from the treatment of multiple soft gluon radiation.

As shown in Eqs. (7)–(9), the effect of multiple gluon radiation, originated from soft gluons connecting the initial and final state gauge links, becomes more important when the final state jet is required to be in the forward region where the kinematic factor  $T \sim \ln \frac{\hat{t}}{\hat{s}}$  becomes large as  $|\hat{t}| \rightarrow 0$ . Consequently, the  $q_{\perp}$  distribution peaks at a smaller value as compared to the case in which the final state jet does not go into the forward region.

Next, we examine the effect of the incoming bottom quark mass to the  $q_{\perp}$  distribution. As shown in Fig. 2(b), a finite bottom quark mass, with  $m_b = 4.75$  GeV, shifts the peak of the  $q_{\perp}$  distribution by about 3–4 GeV as compared to massless case.

As discussed above, the coherence effect of gluon radiation in the initial and final states becomes large when the final state jet falls into more forward (or backward) direction, with a larger absolute value of pseudorapidity. Furthermore, a different prediction in  $q_{\perp}$  would lead to different prediction in the azimuthal angle between the final state jet and the top quark moving directions measured in the laboratory frame. Both of them suggest that we could use the well-known  $\phi^*$  distribution, for describing the precision Drell-Yan pair kinematical distributions [45], to test the effect of multiple gluon radiation in the  $t$ -channel single top quark production. The advantage of studying the  $\phi^*$  distribution is that it only depends on the moving directions (not energies) of the final state jet and top quark.

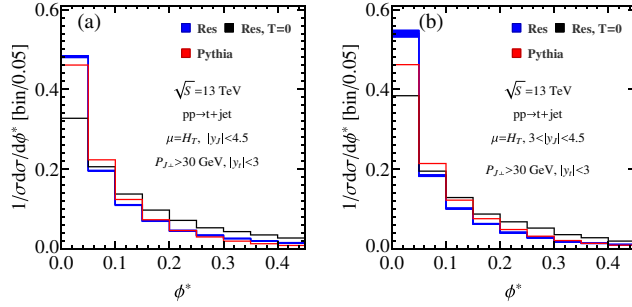


FIG. 3. The normalized distribution of  $\phi^*$  for top quark production at the  $\sqrt{s} = 13$  TeV LHC with  $|y_t| < 3$  and  $P_{J\perp} > 30$  GeV. The resummation and renormalization scales are chosen as  $\mu = \mu_{\text{Res}} = \mu_{\text{ren}} = H_T$ . The blue and black line represents the resummation prediction with and without including the factor  $T$  in Eqs. (7)–(9), respectively. The red lines describe the results from PYTHIA prediction. The blue shaded region represents the scale uncertainties which are varied from  $H_T/2$  to  $2H_T$ .

Hence, it might provide a more sensitive experimental observable when the final state jet falls into forward (or backward) direction. We follow its usual definition and define

$$\phi^* = \tan\left(\frac{\pi - \Delta\phi}{2}\right) \sin\theta_\eta^*, \quad (10)$$

where  $\Delta\phi$  is the azimuthal angle separation in radians between the jet and top quark. The angle  $\theta_\eta^*$  is defined as

$$\cos\theta_\eta^* = \tanh\left[\frac{\eta_J - \eta_t}{2}\right], \quad (11)$$

where  $\eta_J$  and  $\eta_t$  are the pseudorapidities of the jet and top quark, respectively.

As shown in Fig. 3, the predictions of PYTHIA and our resummation calculation differ in the small  $\phi^*$  region, especially for the final state jet falls into more forward (or backward) direction [Fig. 3(b)], which can be caused by a large value of  $\eta_J - \eta_t$ , i.e., in the events with large rapidity gap. In such region, the subleading logarithm terms in the Sudakov factor are important in our resummation calculation. To illustrate this, we also compare to the prediction (shown as black curves in Fig. 3) without the coherence factor  $T$  in Eqs. (7)–(9). It shows that factor  $T$  would change  $\phi^*$  distribution significantly.

Since  $\phi^*$  distribution is sensitive to the color structure of the signal, it could also be used to improve the  $t$ -channel single top quark cross section measurement. In that case, a precise theoretical evaluation of the kinematic acceptance is necessary, which is defined as,

$$\epsilon \equiv \frac{\sigma(\phi^* < \phi^0)}{\sigma}. \quad (12)$$

TABLE I. The predicted kinematic acceptances for the  $\phi^*$  cutoff in the  $t$ -channel single top quark production at the LHC.

$\phi^*$	$< 0.05$	$< 0.1$	$< 0.15$	$< 0.2$	$< 0.25$	$< 0.3$
Res $ y_J  < 4.5$	48%	68%	79%	86%	91%	94%
PYTHIA $ y_J  < 4.5$	46%	68%	81%	88%	93%	96%
Res $3 <  y_J  < 4.5$	54%	72%	83%	89%	93%	96%
PYTHIA $3 <  y_J  < 4.5$	46%	68%	80%	87%	92%	96%

Here,  $\sigma(\phi^* < \phi^0)$  is the cross section after imposing the kinematic cuts, while  $\sigma$  is not. As shown in Table I, if we require the final state jet to be in the forward rapidity region, with  $3 \leq |y_J| \leq 4.5$ , the kinematic acceptance with  $\phi^* < 0.05$  is larger by about 8% in our resummation calculation than the PYTHIA prediction. For  $\phi^* < 0.1$ , they differ by about 4%, and our resummation calculation predicts a larger total fiducial cross section. Currently, the ATLAS and CMS Collaborations have measured the  $t$ -channel single top quark at the 13 TeV LHC, the uncertainty is around 10% [46,47]. If the  $\phi^*$  observable is used to further suppress backgrounds and enhance the signal to backgrounds ratio, the difference found in our resummation and PYTHIA calculations of the fiducial cross section could become important. This will lead to, e.g., different conclusion about the constraints on various  $Wtb$  anomalous couplings, induced by new physics, or the measurement of  $V_{tb}$  [48,49].

In summary, we have presented a transverse momentum resummation calculation to precisely predict the kinematical distributions of the final state jet and top quark produced in the  $t$ -channel single top events at the LHC. We find that it is important to correctly take into account the color coherence effect, induced by soft gluons connecting the initial and final states, which becomes more significant when the final state jet falls into the more forward (or backward) region, where PYTHIA prediction differs the most from our resummation calculation. Motivated by this, we propose to apply the experimental observable  $\phi^*$ , similar to the one used in analyzing the precision Drell-Yan data, to perform precision test of the SM in the production of the  $t$ -channel single top events at the LHC.

## ACKNOWLEDGMENTS

This work is partially supported by the U.S. Department of Energy, Office of Science, Office of Nuclear Physics, under Contract No. DE-AC02-05CH11231; by the U.S. National Science Foundation under Grant No. PHY-1417326; and by the National Natural Science Foundation of China under Grants No. 11275009, No. 11675002, No. 11635001 and No. 11725520. C.-P. Y. is also grateful for the support from the Wu-Ki Tung endowed chair in particle physics.

- [1] S. Dawson, *Nucl. Phys.* **B249**, 42 (1985).  
[2] S. S. D. Willenbrock and D. A. Dicus, *Phys. Rev. D* **34**, 155 (1986).  
[3] S. Dawson and S. S. D. Willenbrock, *Nucl. Phys.* **B284**, 449 (1987).  
[4] C. P. Yuan, *Phys. Rev. D* **41**, 42 (1990).  
[5] E. L. Berger, J. Gao, and H. X. Zhu, *J. High Energy Phys.* **11** (2017) 158.  
[6] N. Kidonakis, *Phys. Rev. D* **74**, 114012 (2006).  
[7] N. Kidonakis, *Phys. Rev. D* **75**, 071501 (2007).  
[8] H. X. Zhu, C. S. Li, J. Wang, and J. J. Zhang, *J. High Energy Phys.* **02** (2011) 099.  
[9] J. Wang, C. S. Li, H. X. Zhu, and J. J. Zhang, *arXiv:1010.4509*.  
[10] N. Kidonakis, *Phys. Rev. D* **83**, 091503 (2011).  
[11] J. Wang, C. S. Li, and H. X. Zhu, *Phys. Rev. D* **87**, 034030 (2013).  
[12] J. C. Collins, D. E. Soper, and G. F. Sterman, *Nucl. Phys.* **B250**, 199 (1985).  
[13] J. C. Collins and D. E. Soper, *Nucl. Phys.* **B193**, 381 (1981); **B213**, 545(E) (1983).  
[14] J. C. Collins and D. E. Soper, *Nucl. Phys.* **B197**, 446 (1982).  
[15] H. X. Zhu, C. S. Li, H. T. Li, D. Y. Shao, and L. L. Yang, *Phys. Rev. Lett.* **110**, 082001 (2013).  
[16] H. T. Li, C. S. Li, D. Y. Shao, L. L. Yang, and H. X. Zhu, *Phys. Rev. D* **88**, 074004 (2013).  
[17] R. Zhu, P. Sun, and F. Yuan, *Phys. Lett. B* **727**, 474 (2013).  
[18] P. Sun, C. P. Yuan, and F. Yuan, *Phys. Rev. Lett.* **114**, 202001 (2015).  
[19] P. Sun, C. P. Yuan, and F. Yuan, *Phys. Rev. Lett.* **113**, 232001 (2014).  
[20] P. Sun, C. P. Yuan, and F. Yuan, *Phys. Rev. D* **92**, 094007 (2015).  
[21] P. Sun, C. P. Yuan, and F. Yuan, *Phys. Lett. B* **762**, 47 (2016).  
[22] P. Sun, J. Isaacson, C. P. Yuan, and F. Yuan, *Phys. Lett. B* **769**, 57 (2017).  
[23] B.-W. Xiao and F. Yuan, *Phys. Lett. B* **769**, 57 (2017).  
[24] F. Landry, R. Brock, G. Ladinsky, and C. P. Yuan, *Phys. Rev. D* **63**, 013004 (2000).  
[25] F. Landry, R. Brock, P. M. Nadolsky, and C. P. Yuan, *Phys. Rev. D* **67**, 073016 (2003).  
[26] P. Sun, C. P. Yuan, and F. Yuan, *Phys. Rev. D* **88**, 054008 (2013).  
[27] S. Dulat, T.-J. Hou, J. Gao, M. Guzzi, J. Huston, P. Nadolsky, J. Pumplin, C. Schmidt, D. Stump, and C. P. Yuan, *Phys. Rev. D* **93**, 033006 (2016).  
[28] M. A. G. Aivazis, F. I. Olness, and W.-K. Tung, *Phys. Rev. D* **50**, 3085 (1994).  
[29] M. A. G. Aivazis, J. C. Collins, F. I. Olness, and W.-K. Tung, *Phys. Rev. D* **50**, 3102 (1994).  
[30] J. C. Collins, *Phys. Rev. D* **58**, 094002 (1998).  
[31] M. Kramer, F. I. Olness, and D. E. Soper, *Phys. Rev. D* **62**, 096007 (2000).  
[32] P. M. Nadolsky, N. Kidonakis, F. I. Olness, and C. P. Yuan, *Phys. Rev. D* **67**, 074015 (2003).  
[33] A. Belyaev, P. M. Nadolsky, and C. P. Yuan, *J. High Energy Phys.* **04** (2006) 004.  
[34] S. Berge, P. M. Nadolsky, and F. I. Olness, *Phys. Rev. D* **73**, 013002 (2006).  
[35] A. Mukherjee and W. Vogelsang, *Phys. Rev. D* **86**, 094009 (2012).  
[36] M. Dasgupta and G. P. Salam, *Phys. Lett. B* **512**, 323 (2001).  
[37] M. Dasgupta and G. P. Salam, *J. High Energy Phys.* **03** (2002) 017.  
[38] A. Banfi and M. Dasgupta, *J. High Energy Phys.* **01** (2004) 027.  
[39] J. R. Forshaw, A. Kyrieleis, and M. H. Seymour, *J. High Energy Phys.* **08** (2006) 059.  
[40] P. Sun, C. P. Yuan, and F. Yuan (to be published).  
[41] T. Sjostrand, S. Mrenna, and P. Z. Skands, *Comput. Phys. Commun.* **178**, 852 (2008).  
[42] C. Patrignani *et al.* (Particle Data Group), *Chin. Phys. C* **40**, 100001 (2016).  
[43] C. Balazs and C. P. Yuan, *Phys. Rev. D* **56**, 5558 (1997).  
[44] J. M. Campbell, R. K. Ellis, and W. T. Giele, *Eur. Phys. J. C* **75**, 246 (2015).  
[45] A. Banfi, S. Redford, M. Vesterinen, P. Waller, and T. R. Wyatt, *Eur. Phys. J. C* **71**, 1600 (2011).  
[46] CMS Collaboration (2016).  
[47] M. Aaboud *et al.* (ATLAS), *J. High Energy Phys.* **04** (2017) 086.  
[48] Q.-H. Cao, B. Yan, J.-H. Yu, and C. Zhang, *Chin. Phys. C* **41**, 063101 (2017).  
[49] Q.-H. Cao and B. Yan, *Phys. Rev. D* **92**, 094018 (2015).